Earthquakes and Structures, *Vol. 17, No. 2 (2019) 221-232*
DOI: https://doi.org/10.12989/eas.2019.17.2.221

Strengthening RC frames subjected to lateral load with Ultra High-Performance fiber reinforced concrete using damage plasticity model

Sai Kubair Kota[1a], J.S. Kalyana Rama[*2,3] and A. Ramachandra Murthy[4b]

[1]*Department of Civil Engineering, Delft University of Technology, Delft, 2628, Netherlands*
[2]*Department of Civil Engineering, Birla Institute of Technology & Science, Pilani-Hyderabad Campus, Shameerpet, Hyderabad-500078, India*
[3]*Vignana Bharathi Institute of Technology, Ghatkesar, Hyderabad-501301, India*
[4]*Fatigue and Fracture Laboratory, Structural Engineering Research Center (CSIR-SERC), Taramani, Chennai-600113, India*

(Received February 1, 2019, Revised May 23, 2019, Accepted June 6, 2019)

Abstract. Material non-linearity of Reinforced Concrete (RC) framed structures is studied by modelling concrete using the Concrete Damage Plasticity (CDP) theory. The stress-strain data of concrete in compression is modelled using the Hsu model. The structures are analyzed using a finite element approach by modelling them in ABAQUS / CAE. Single bay single storey RC frames, designed according to Indian Standard (IS):456:2000 and IS:13920:2016 are considered for assessing their maximum load carrying capacity and failure behavior under the influence of gravity loads and lateral loads. It is found that the CDP model is effective in predicting the failure behaviors of RC frame structures. Under the influence of the lateral load, the structure designed according to IS:13920 had a higher load carrying capacity when compared with the structure designed according to IS:456. Ultra High Performance Fiber Reinforced Concrete (UHPFRC) strip is used for strengthening the columns and beam column joints of the RC frame individually against lateral loads. 10mm and 20mm thick strips are adopted for the numerical simulation of RC column and beam-column joint. Results obtained from the study indicated that UHPFRC with two different thickness strips acts as a very good strengthening material in increasing the load carrying capacity of columns and beam-column joint by more than 5%. UHPFRC also improved the performance of the RC frames against lateral loads with an increase of more than 3.5% with the two different strips adopted. 20 mm thick strip is found to be an ideal size to enhance the load carrying capacity of the columns and beam-column joints. Among the strengthening locations adopted in the study, column strengthening is found to be more efficient when compared with the beam column joint strengthening.

Keywords: strengthening; damage plasticity model; ABAQUS; UHPFRC; lateral load; beam-column joint

1. Introduction

The main aim of a column is to transfer all the loads carried by the structural components to the foundation. The requirement of a joint is to allow the members to attain their maximum achievable load. But these columns and the beam column joints of a structure are weak against lateral loads and a special care has to be taken that they have adequate strength, stiffness and ductility to resist these loads. Also, these loads which affect the main components of the structure are unpredictable.

So in the present study, one such effective strengthening material for RC frames against lateral loads is proposed and behavior of the RC frame after strengthening is analyzed.

1.1 Various material models for simulating the nonlinear behavior of concrete:

Smeared cracking model

This model is suitable for simulating the behavior of concrete subjected to monotonic loading with low confining pressures i.e., not exceeding four to five times the uniaxial compressive stress). It assumes the main failure mechanism to be smeared cracking, which is assumed to occur when the stresses reach failure surface (crack detection surface) defined in the *p*-*q* plane, where, p^- and q^- are the first and second stress invariants of the deviatoric stress respectively. Smeared cracking implies that individual micro-cracks at each numerical integration point are not tracked. The crack affects material stiffness and stresses at that integration point. The model utilizes a multi-axial plasticity model for compressive stresses and a two parameter Drucker-Prager yield surface, associated flow rule and isotropic hardening. The associative flow rule simplifies the actual behavior of concrete and over estimates the inelastic strain when strained beyond the ultimate stress.

Brittle cracking model

Brittle crack simulation depends on rupture parameters of concrete and is similar to discrete crack analysis. It is also applicable to other brittle materials, such as ceramics and brittle rocks; however is primarily for modeling plain concrete. In brittle mode, micro-cracks merge to form discrete regions of localized deformation, and in ductile mode micro-cracks form almost uniformly throughout the material i.e., non-localized deformation. Brittle behavior is associated with shears, cleavage, and mixed fracture

∗Corresponding author, Assistant Professor
E-mail: kalyan@hyderabad.bits-pilani.ac.in
[a]MS Graduate Student
[b]Principal Scientist

http://www.techno-press.com/journals/eas&subpage=7
ISSN: 2092-7614 (Print), 2092-7622 (Online)

mechanisms observed under tension and tension-compression stress states, generally involving softening of the material. The ductile behavior is associated with dispersed micro-cracking mechanism observed under compression stress states and generally involves hardening of the material. The brittle cracking model only accounts for brittle behavior, though quite a simplification, is justified in many applications. The assumption is that the material is linear elastic in compression zone.

Concrete damaged plasticity model

The typical behavior of concrete can be determined using the Concrete Damage Plasticity (CDP) Model which is available in ABAQUS, a FEA software. CDP is a constitutive continuum based model that combines plasticity and damage mechanics. It is a modified form of the Drucker-Prager strength hypothesis in which the failure of a material is determined by the non-dilatational strain energy and the failure surface is assumed to be of conical shape with circular cross section (not completely consistent with the real behavior of concrete). In CDP, various parameters (scalar damage variables) are used to describe the behavior of concrete in terms of yield surface and flow.

Dilation/dilatancy angle (β or ψ): The angle of inclination of the failure surface towards the hydrostatic axis, measured in the meridional plane. Physically, it is interpreted as the internal friction angle of concrete, which describes the extent of volume change experienced by concrete as cracks. (~ 36° to 40° is generally adopted for concrete). Low dilation angles overestimate post-elastic stiffness. (~10 degrees, inadequate confinement). High dilation angles underestimate post-elastic stiffness. It is measured in p-q plane (in degrees)

Flow potential eccentricity(ϵ): It describes the shape of the plastic potential surface in the model, which is a hyperbola. It is the rate at which the function (hyperbola) approaches the asymptote (the flow potential tends to a straight line as the eccentricity tends to zero). It can be calculated as the ratio of tensile to compressive strength. (~0.1)

fb_0/fc_0: It is the ratio of biaxial compressive yield stress to uniaxial compressive yield stress (~1.16)

K_c: It is the ratio of the second stress invariant on the tensile meridian to that on the compressive meridian for the yield function, at initial yield for any value of the pressure invariant such that maximum principal stress is negative. The failure cross section need not be a circle and its shape is determined by this parameter. (~ 2/3).

Viscosity parameter (υ or μ): It is utilized for the visco-plastic regularization of constitutive equations of concrete. The adjustment (μ) should be (>0) greater than zero such that the ratio of problem's time step to μ tends to infinity. Hence, visco-elastic materials should have μ value as small as possible. For non-visco-elastic materials, the value should be 0.

The above 5 parameters along with stress-strain behavior of concrete in tension and compression are the input parameters for CDPM in ABAQUS. Besides this, compression damage (d_c) and tension damage (d_t) input is also to be defined (yield stress vs. inelastic and cracking strain).

1.2 Review of existing literature

Sümer *et al* (2015) studied about different parameters involved in the CDP model for an RC beam. The results from this study indicated that CDP model can be used to model the damage behavior of concrete. Jankowaik *et al* (2005) worked on identification of parameters of the concrete damage plasticity (CDP) model.

A comparative study was performed on predicting the behavior of notched beams with different CDP parameters and static loading conditions. The results obtained from the study indicated that CDP model is successfully able to predict the damage behavior of concrete.

Lin *et al* (2004) performed nonlinear static and dynamic analyses on RC frame structures with emphasis on the material modeling. They focused on the influence of material modeling on the behavior of RC structures and their nonlinear analysis. Two material models are considered: Drucker-Prager & CDP models with strain hardening effects. Results from this study showed that different outputs are obtained for different material models used. It is also observed that the non-linear material modelling predicted the behavior of the RC frame accurately.

Tayeh *et al.* (2013) worked on reviewing the Utilization of UHPFRC for rehabilitation. It is mentioned that in some zones of stress concentration, rehabilitation or strengthening of the structure is essential to sustain these unexpected loads. The results of this study mention that UHPFRC is an excellent material for repair, strengthening and rehabilitation because of its enhanced durability over other concretes and its low porosity characteristics.

Lampropoulos *et al.* (2015) assessed the efficiency of strengthening Reinforced Concrete (RC) beam using UHPFRC. Full scale experimental study on the strengthened beams had been performed using three different strengthening techniques. The results obtained from the study indicated that UHPFRC is efficient in improving the load carrying capacity of the RC beam in case of all strengthening techniques. Prem *et al*. (2015) studied about the flexural behavior of damaged RC beam using UHPFRC. In this study, RC beams were strengthened with UHPFRC casted in the form of strip. The results obtained after testing these beams indicated that UHPFRC is efficient in improving the strength properties of damaged RC beam to a great extent.

Rahman *et al.* (2005) worked on the recent applications and research on UHPFRC. It is stated in the study that the UHPFRC is characterized as a material possessing good strength and durability characteristics. Work of different researchers on this concrete resulted in a variety of UHPFRCs such as the Compact Reinforced Concrete, Macro Defect Free Concrete, and Densified Small Particles Concrete etc. There are various applications of UHPFRC documented in this study such as the construction of high rise structures, retrofitting and rehabilitation of structures etc. Chen *et al.* (2011) modelled the structural performance of UHPFRC I-Girders. In this the structural behavior of UHPFRC is modelled using the CDP model based on a finite element package. From the results obtained, it is concluded that the CDP model is efficient in replicating both the linear and non-linear responses of concrete. (Ashish *et al.* 2014) investigated the behavior of beam-column joint retrofitted with FRP wrapping under seismic loading. The wrapping appreciably increased the stiffness, lateral strength, and ductility of the member whose joints were initially highly vulnerable to fail due to earthquake loading. (Truong *et al.* 2017) studied the seismic response of RC columns retrofitted with concrete jacketing, steel jacketing, CFRP wrapping, etc. Half scale RC columns were subjected to earthquake excitations and axial loads experimentally. The capacities of the structures were analyzed on the basis of various factors like stiffness, dissipation ratio, drift capacity, etc. This strategy was shown to successfully improve the performance of the structures under seismic load by increasing the load carrying and non-linear failure deformation capacity, and ductility.

Tsonos (2009) proposed new earthquake resistant methodology to strengthen old reinforced concrete structures using steel fiber high strength concrete jackets. He proved that the proposed methodology is superior to FRP jacketing and can be easily adopted. Chalioris (2011, 2013) studied the influence of addition of steel fibers in RC beams subjected to cyclic deformation under predominant shear. Results indicated that the addition of fibers enhanced the shear strength and energy absorption capacity of the beam. Chalioris and Panagiotopoulos (2018) proposed a new numerical approach to study the behaviour of steel fiber reinforced concrete sections with arbitrary geometry. They have employed a new stress-strain model to evaluate the bending moment and curvature curves numerically. They have validated their results with the experimental values and results indicated that the proposed model provided a better and accurate compressive and tensile stress-strain curves.

Sümer *et al.* (2015) further suggested an equation for damage parameters to capture damage behavior of concrete. A numerical modeling strategy was created by checking the model sensitivity against fracture parameters and mesh density. The results of the numerical model were verified through lab testing and proved to be sufficiently accurate. The same was confirmed by Michal *et al.* (2015) through application and calibration of the CDPM parameters for assessing the damage in an RC frame. Studies were conducted on punching shear failure mode of concrete caused by static and pseudo-dynamic loading conditions. Since the existing database of punching shear mode of failure in concrete based on empirical data is not sufficient to encompass all aspects of the transfer mechanism, Genikomsou and Polak (2015) worked on simulating and analyzing the responses of five concrete slabs, using CDP model with material parameter calibration, through ABAQUS. In addition to the study conducted on punching shear failure, the effect of quasi-static cyclic lateral load on the behavior and failure mode of a conventional RC beam column joint was investigated by Fadwa *et al.* (2014). Syrian design code was adopted and samples with interior and exterior joints are considered. Comparative studies were done on conventional joints and wider joints. Results indicated that wider joints have better hysteretic behavior compared to conventional ones. Additionally, the wider joints failed by a flexural hinging mechanism instead of failing in a brittle mode, which generally occurs due to torsion. A time history analysis was conducted which was in par with data and results from experimental testing. Numerous approaches to elucidate the performance of these masonry infill walls subjected to dynamic loads have been presented by Ali Shah *et al.* (2013).

From the review of literature, it can be noted that UHPFRC serves a good material in terms of both strength and durability. Due to its ductile nature it can be used for strengthening, retrofitting and rehabilitation of structures successfully. In comparison with the conventional concrete, UHPFRC is a highly durable material. The CDP model is efficient in predicting the non-linear behavior of RC framed structures and UHPFRC. UHPFRC is used for strengthening and retrofitting RC beams but there is no literature available on strengthening RC frames using UHPFRC. So in the present study, an effort is made to study the non-linear behavior of RC frames designed as per IS:456 and IS:13920 using the Hsu model as an input for the CDP model. The failure behavior and the maximum capacity of these structures subjected to lateral loads is studied. Then, these RC frames are strengthened using UHPFRC using two techniques: column and beam column joint strengthening. The failure behavior of the UHPFRC strengthened RC frames and the efficiency of UHPFRC in strengthening the RC frames are assessed.

2. Numerical modelling of concrete using the CDP model

2.1 Compressive behavior of concrete

2.1.1 Calculating the elastic modulus of concrete

According to IS: 456:2000, the elastic modulus of a particular grade of concrete can be calculated as mentioned in Eq. (1).

$$E_{cm} = 5000(f_{ck})^{0.5} \tag{1}$$

where, f_{ck} is the characteristic compressive strength of concrete.

2.1.2 Hsu & Hsu model

This model can generate the stress strain curve of concrete up to a point in the descending part where the stress is equal to 0.3 times the peak stress. The yield stress is equal to half the peak stress value. This theory can model concrete with strengths equal to 62 MPa. This model can be used even for modelling high strength concretes with minor changes. The formulations involved in this model for normal strength concretes are as mentioned in Eqs. (2)-(3).

$$\sigma_c = E_{cm}\varepsilon_c \text{ - Up to the yield point} \tag{2}$$

$$\sigma_c = \left(\frac{\beta\frac{\varepsilon_c}{\varepsilon_0}}{\beta-1+\left(\frac{\varepsilon_c}{\varepsilon_0}\right)^{\beta}}\right)\sigma_{cu} \text{ - After the yield point} \tag{3}$$

where ε_c and ε_0 are the strain at any point and strain at peak stress in concrete respectively, σ_{cu} is the peak stress in concrete in kip/in^2 and β is a parameter which decides the nature of the stress-strain curve. These parameters can be calculated as given in Eqs. (4)-(5).

$$\varepsilon_0 = 8.9 \times 10^{-5}\sigma_{cu} + 2.114 \times 10^{-3} \tag{4}$$

$$\beta = \frac{1}{1 - \left(\frac{\sigma_{cu}}{E_{cm}\varepsilon_0}\right)} \tag{5}$$

2.2 Tensile behavior of concrete:

The maximum tensile strength of concrete is calculated based on the formula mentioned in the EUROCODE 2 which is as mentioned in Eq. (6).

$$f_{ctm} = 0.3 \times f_{ck}^{2/3} \tag{6}$$

where, f_{ctm} is the maximum tensile strength of concrete.

This value is given as an input in the concrete damage plasticity (CDP) model in the tension part and the maximum cracking strain value of concrete is taken as a constant equal to 0.01. These two values are given as an input in the tension part of the CDP model.

2.3 Predicting the damage variables in the CDP model

The damage variable in compression (d_c) is calculated based on the damage theory as the ratio of inelastic strain in compression (crushing strain) at a particular point to that of the maximum strain allowed in concrete as mentioned in Eq. (7).

$$d_c = \frac{\varepsilon_c^{\sim in}}{\varepsilon_c^{max}} \tag{7}$$

where, $\varepsilon_c^{\max}$ is the maximum strain in compression that can be allowed in concrete calculated as per the Hsu & Hsu model. The maximum value of damage variable in tension (d_t) is again taken as a constant which is equal to 0.9 and the damage value at the yield stress will be equal to zero.

3. Selecting the RC frame for analysis

The RC frame chosen is a single bay and single storey space framed structure. The height of the frame is considered to be 3.5 m and plan dimension of the structure is 4 m. The shape and dimensions of the RC frame are shown in Fig. 1.

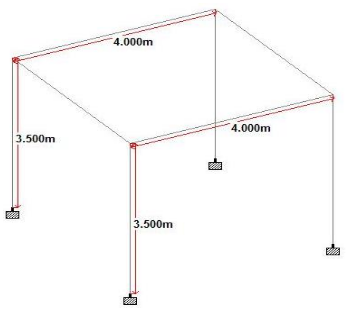

Fig. 1 RC frame considered for the analysis

Table 1 Beam reinforcement details in GLDS

S.No	Grade of Concrete (MPa)	Top Reinf. (mm^2)	Bottom Reinf. (mm^2)	Stirrups
1	M20			
2	M25			
3	M30	384.34 (4-12ϕ)	384.34 (4-12ϕ)	8 mm ϕ @200 mm
4	M35			
5	M40			

Table 2 Column reinforcement details in GLDS

S.No	Grade of Concrete (MPa)	Main Reinf. (mm^2)	Links
1	M20	490 (4 - 16 ϕ)	
2	M25	470 (4 - 16 ϕ)	
3	M30	456 (4 - 16 ϕ)	8 mm ϕ@ 200 mm
4	M35	447 (4 - 12 ϕ)	
5	M40	439 (4 - 12 ϕ)	

4. Designing and modelling the RC frame according to IS:456

The RC frame is designed using the STAAD PRO V8I based on IS: 456:2000, the Indian standard for RCC structural design. Grades of concrete considered for analysis are M20, M25, M30, M35 and M40. The cross sectional dimensions of both beams and columns considered for the design purpose are 450 mm×450 mm. The load details that are considered for designing the RC frame are as follows:

• ***Dead loads (DL):***
i. Self Weight of the members of the structure.
ii. Wall load=12 KN/m.

• ***Live loads (LL):***
i. Floor load=3 KN/m^2.
• Load combination=1.5 (DL + LL) according to IS: 1893 - Part II.

4.1 RCC Design Details of the Gravity Loads Designed Structure (GLDS)

The details of reinforcement that has to be provided inside beams and columns for different grades of concrete starting from M20 to M40 are given in Tables 1-2 respectively.

( ) - Inside this represents the reinforcement provided in the member.

4.2 Finite element modelling of the RC frame

The RC frame designed in STAAD PRO V8I is modelled in ABAQUS / CAE and analyzed based on a finite element approach. The assembly of different components of the RC frame are as shown in the Figs. 2 and 3 respectively. Concrete is meshed using the C3D8R (eight noded linear brick) element and the reinforcement (steel bars and stirrups) is meshed using the T3D2 (two noded truss) element. In this study, the size of the truss element used for meshing the reinforcement is kept as a constant equal to 20.

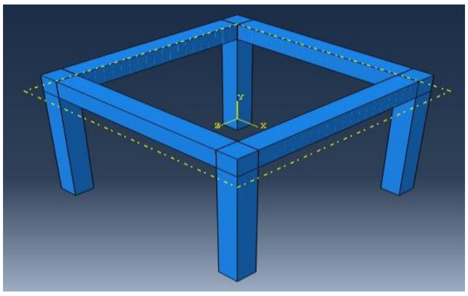

Fig. 2 Assembly of beams and the columns

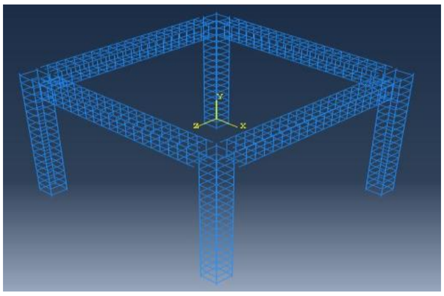

Fig. 3 Assembly of main rebars and stirrups

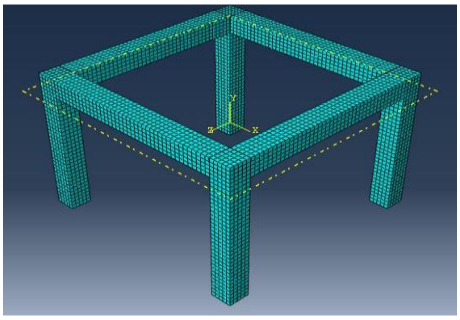

Fig. 4 Meshing of Concrete

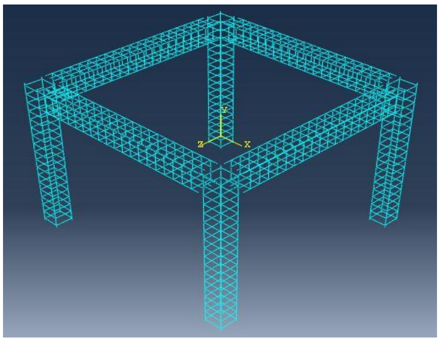

Fig. 5 Meshing the reinforcement

The element size used for meshing the concrete part is varied for performing the mesh convergence studies. The meshing of concrete and steel is as shown in the Figs. 4 and 5.

5. Assessing the behavior of the structure under gravity loads

5.1 Evaluating the maximum load carrying capacities of GLDS

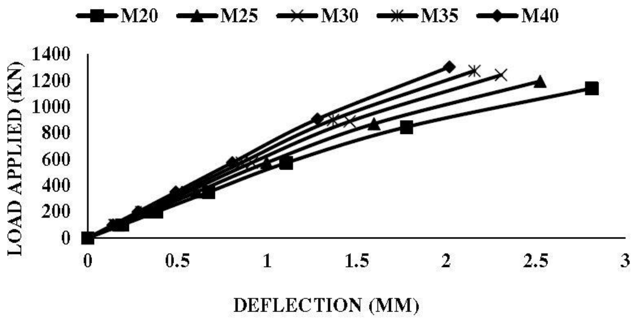

Fig. 6 Load vs. deflection behavior of GLDS for 1000 KN load

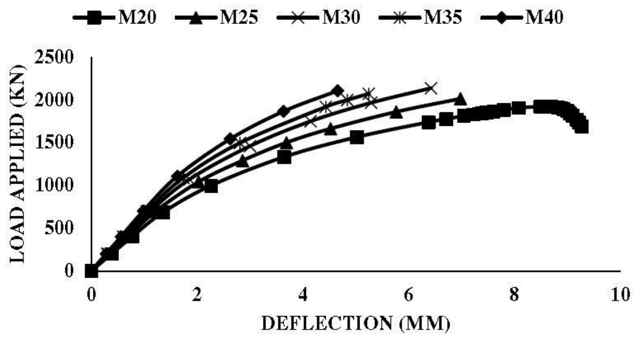

Fig. 7 Load vs. deflection behavior of GLDS for 2000 KN load

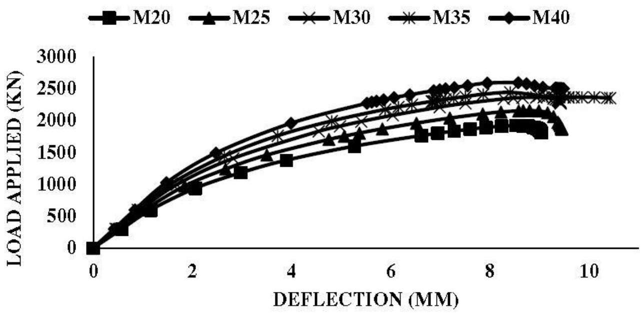

Fig. 8 Load vs. Deflection behavior of GLDS for 3000 KN load

To assess the maximum load carrying capacity of GLDS, a trial and error based approach has been adopted starting with a total load of 1000 KN, 2000 KN, 3000 KN & 4000 KN. This load is applied on the beams GLDS by distributing the total load among all the beams equally. The analysis has been performed on all the structures with different grades of concrete and a random mesh size of 100 has been used to mesh concrete. The responses of the structure for different grades of concrete and for different static loads applied from 1000KN to 4000KN are shown in Figs. 6-9 respectively.

From the analysis, it can be inferred that all the structures failed for 3000 KN total load which means that this is the maximum gravity load carrying capacity of the structures. It can also be observed from Fig. 9, that a similar load deflection behavior is obtained even at a load of 4000 KN which means that the behavior of the structures does not depend on the applied load but on the non-linear behavior of the concrete and steel.

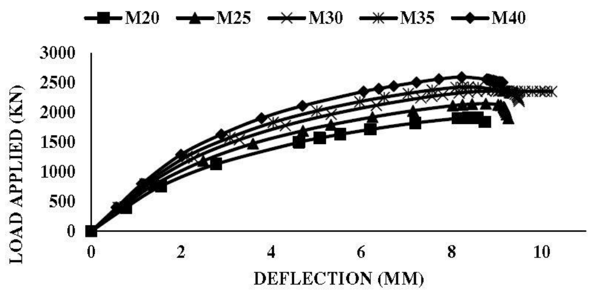

Fig. 9 Load vs. Deflection behavior of GLDS for 4000 KN load

5.2 Mesh convergence studies

As the ultimate load carrying capacities of the structures are known, a mesh convergence study has been performed on all the structures. For this concrete is meshed with different meshes with different sizes starting from 50, 60, 70, 80, 90 and 100. The mesh size of steel is kept as a constant equal to 20. Maximum deflection of the structure is used as a parameter for analyzing the mesh convergence. The maximum deflections obtained after the mesh convergence analysis for structures with different grades of concrete are shown in Fig. 10.

From Fig. 10, it can be noted that for all the structures with different grades of concrete, the maximum deflection values stay close to each other in case of meshes sizes equal to 80, 90 & 100. For, other mesh sizes the results abruptly vary which is not acceptable. So a mesh size of 80 has been used for meshing the concrete in the further part of the study.

5.3 Load-deflection behavior of the structures after mesh convergence studies

After performing the mesh convergence studies, the structure is again analyzed for its load-deflection behavior under static load. A mesh size of 80 has been used to mesh concrete and steel with a constant element size of 20. The total load applied on the structure is 3000 KN which is equally distributed on the beams. The load-deflection behaviors of the structure with different grades of concrete, obtained after conducting the mesh convergence analysis are shown in Fig. 11.

It can be inferred that as the grade of concrete increases, the load carrying capacity of the structure increases accordingly. All the structures reached their ultimate load carrying capacity which could be observed from the softening behavior of these curves after the peak point.

5.4 Analysis of first failure loads

The first failure loads of concrete and steel obtained after performing the analysis is as shown in Fig. 12. As the grade of concrete increases, the cracking load of concrete and steel also increased. The failure patterns in concrete and steel due to the applied gravity load are as shown in the Figs. 13 and 14.

First crack is seen near the beam-column joint due to high stress concentration, followed by the complete failure of the joint. Then the beams failed in flexure and the first crack in beams appeared at the centre of the beam. Then a small crack at the bottom part of columns is seen due to the tensile stress generated. Reinforcement started yielding first at the beam column joint region followed by the yielding of flexural reinforcements in the beam which made the structure reach its ultimate load and finally fail.

6. Designing the RC frame according to IS:13920

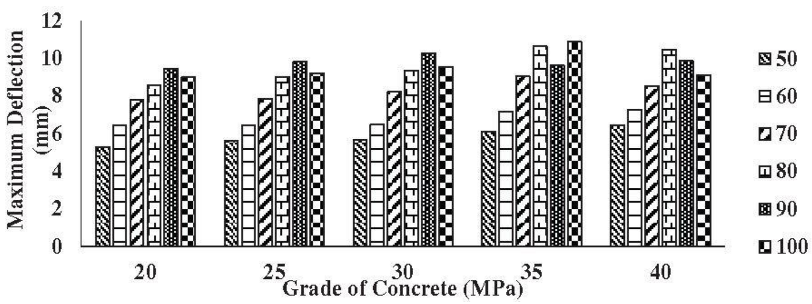

Fig. 10 Maximum deflections of GLDS with different grades of concrete

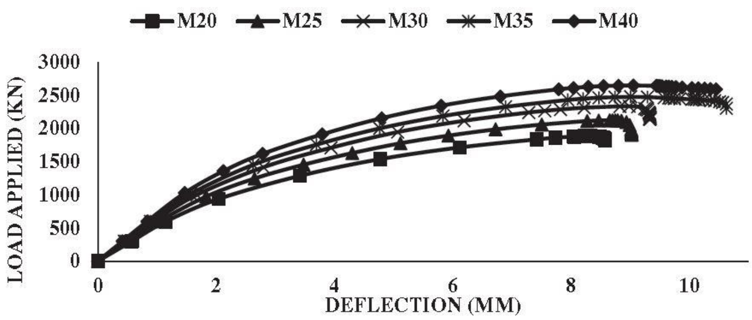

Fig. 11 Load vs. deflection behavior of GLDS after the mesh convergence studies

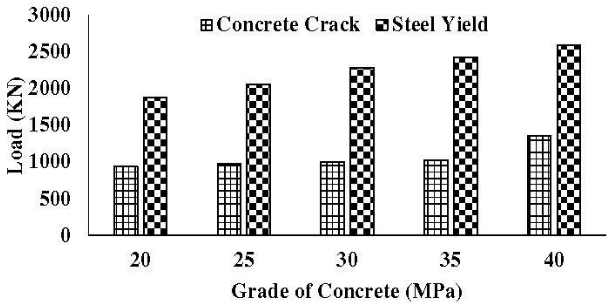

Fig. 12 First failure loads of different grades of concrete in GLDS due to **gravity load**

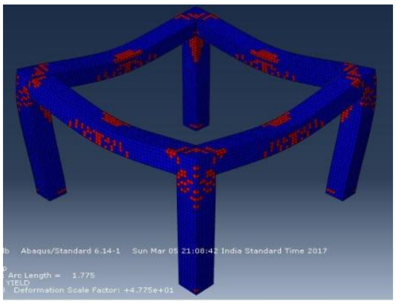

Fig. 13 Cracking of concrete in GLDS

Fig. 14 Yielding of steel in GLDS

The RC frame is designed using STAAD PRO V8I based on IS: 13920:2016, the Indian standard for seismic RCC structural design. This structure is termed as Earthquake Loads Designed Structure (ELDS). Grade of concrete considered for analysis is M40 alone as most of the high rise structures are adopting M40 grade of concrete. The cross sectional dimensions of both beams and columns considered for the design purpose are 450 mm×450 mm. The parameters of the RC frame considered according to IS: 1893-2002 for the earthquake resistant design in STAAD are:

i. Earthquake Zone: V.
ii. Structure type: Special moment resisting RC frame.
iii. Structure is considered to be a highly important structure.
iv. Soil type: Loose soil
v. Damping ratio: 5%.

The occurrence of the earthquake is assumed to be in all the four possible directions i.e., + X, - X, + Z & - Z. The corresponding earthquake load definitions are assigned to the structure.

Table 3 Beam reinforcement details in ELDS

S.No	Grade of Concrete (MPa)	Top Reinf. (mm^2)	Bottom Reinf. (mm^2)	Stirrups
1	M40	691.28 (4-16ϕ)	691.28 (4-16ϕ)	8 mm ϕ @100 mm

Table 4 Column reinforcement details in ELDS

S.No	Grade of Concrete (MPa)	Main Reinf. (mm^2)	Links
1	M40	1620 (4-25ϕ)	8 mm ϕ@ 100 mm

The static load details used for this design are as follows:

- **Dead loads (DL):**
  i. Self-Weight of the members of the structure.
  ii. Wall load=12 KN/m.

- **Live loads (LL):**
  i. Floor load=3 KN/m^2.

Based on IS: 1893 - Part- II, all the load combinations are generated depending on the nature of the general load cases that are applied on the structure.

6.1 RCC design details of ELDS

The details of reinforcement that has to be provided inside the RC frame for M40 grade of concrete are given in Tables 3-4.

( ) - Represents the reinforcement provided in the member.

6.2 Finite element modelling of ELDS

ELDS is modelled in ABAQUS/CAE in a similar way as modelled in the case of GLDS and analyzed based on the finite element approach. Assuming the mesh convergence analysis to be almost the same as in the case of GLDS, a constant element size of 80 is also maintained throughout the analysis ELDS. The reinforcement assembly, mesh details of the structure and the reinforcement inside ELDS are as shown in the Figs. 15-17.

7. Lateral load behaviors of GLDS and ELDS

7.1 Lateral load carrying capacities of the structures

To find out the maximum lateral load carrying capacities of GLDS and ELDS, they are subjected to a lateral load at the joints and a displacment control method of loading is adopted. The concrete part of the strcutures is meshed with an element size of 80 and reinforcement using the same element size of 20. The lateral load vs. lateral displacement behaviors of these structures are as shown in the Fig. 18.

It can be observed that ELDS has a higher potential of taking lateral load than GLDS because of its ductile nature. The ultimate lateral load of ELDS is almost double to that of the GLDS which reveals that structural ductility is a very important parameter in improving the lateral load carrying capacity of the structure.

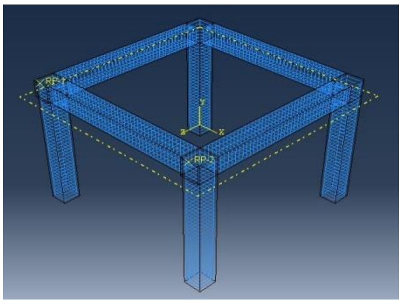

Fig. 15 Reinforcement assembly in ELDS

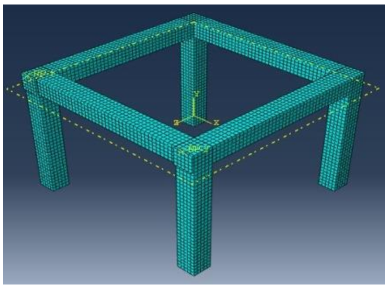

Fig. 16 Meshing of concrete in ELDS

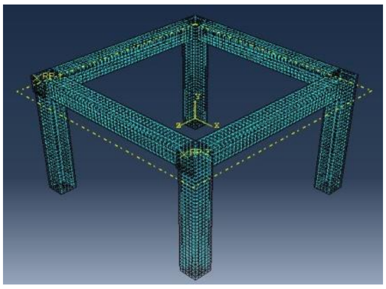

Fig. 17 Meshing of steel in ELDS

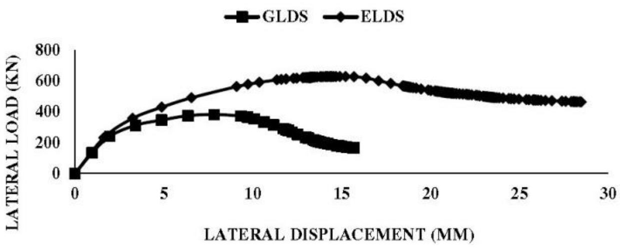

Fig. 18 Lateral Load vs. displacement behavior of GLDS and ELDS

7.2 Analysis of first failure loads

The first failure behaviors of concrete and steel in these stuctures when subjected to lateral load are as shown in the Fig. 19.

It can be noted that both concrete and steel failed when a higher load is applied in case of ELDS when compared with GLDS. The failure patterns observed in concrete and steel of these structures when a lateral load is applied on the structure are as shown in the Figs. 20 and 21.

7.3 Observations from the failure patterns:

From the failure patterns, it is clear that the cracks in

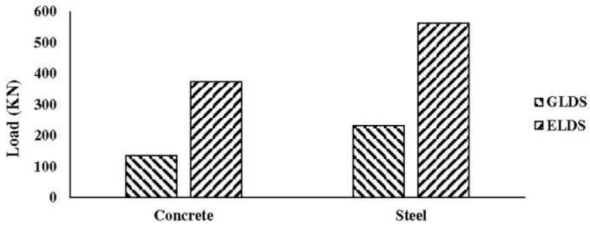

Fig. 19 First failure loads of concrete and steel in GLDS and ELDS

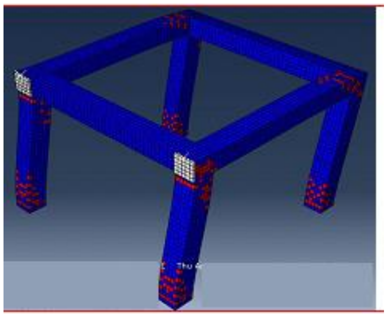

Fig. 20 Cracking of concrete in the structures

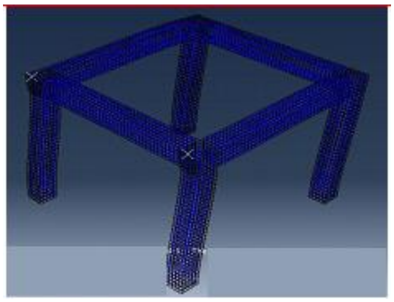

Fig. 21 Yielding of steel in the structures

concrete first started at the base of the columns and then propogated further to the inner side of the column near the beam column joint. After a certain time, some cracks started at the beam column joints and these cracks also propogated further to the edges of the columns. Yielding in steel is recoreded at the base of the column first and then at the beam column joints.

8. Strengthening material (UHPFRC)

UHPFRC has higher performance in terms of strength and workability when compared with that of normal concrete. The first reason is that they do not contain any aggregate in them and majority of the material inside them is a combination of cementitious materials like cement, micro silica, silica fumes etc. The second reason is the presence of fibers which makes it more ductile when compared with other concretes. In view of these advantages, UHPFRC is used to strengthen columns and beam column joints of GLDS and ELDS which are highly vulnerable to lateral loads in the present study. This material is modelled using the CDP model. The data required for modelling UHPFRC in ABAQUS using the CDP model is taken from Prem *et al*. (2015).

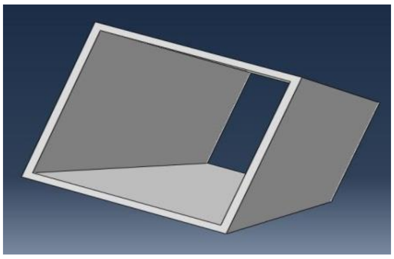

Fig. 22 Shape of UHPFRC strip used for column strengthening

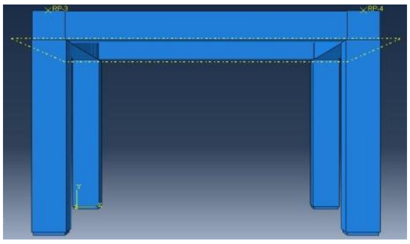

Fig. 23 Assembly of UHPFRC with the structures

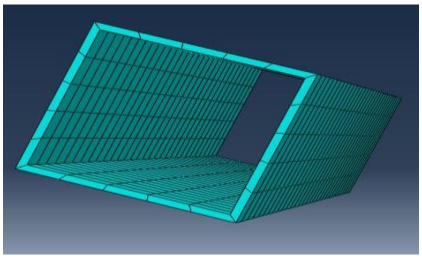

Fig. 24 Meshing the UHPFRC strip

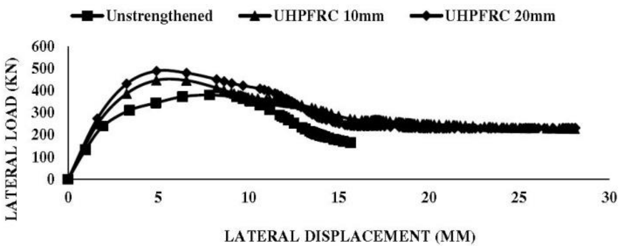

Fig. 25 Lateral load vs. displacement behavior of GLDS before and after column strengthening

9. Behavior of UHPFRC strengthened GLDS and ELDS against lateral loads

9.1 Analyzing the behavior of RC frame with columns strengthened using UHPFRC strip

The columns of the GLDS and ELDS are strengthened using UHPFRC strips of thicknesses equal to 10 mm and 20 mm. These strips are modelled as hollow members of inner dimensions equal to the dimension of the columns and thicknesses equal to 10 mm and 20 mm. These strips are wrapped around the column of the RC frame as a jack*et al*ong its height. The details of the strip models are shown in the Fig. 22.

These strips are attached to all the columns of GLDS and ELDS. The bonding between the strip and the column is neglected for the current study. All the UHPFRC strips

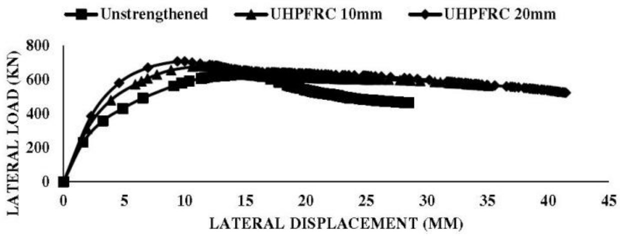

Fig. 26 Lateral Load vs. Displacement behavior of ELDS before and after column strengthening

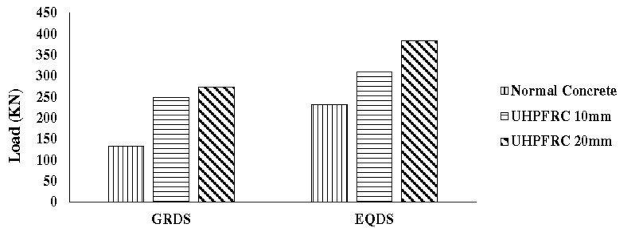

Fig. 27 First failure loads of materials in structures after column strengthening

used for strengthening the RC frame in the present study are meshed using the eight noded cubic element (C3D8R) with an element size equal to 80. The assembly of the strip with the frames and the mesh details of the strips are shown in the Figs. 23 and 24.

The lateral load vs. displacement behavior of GLDS and ELDS for different thicknesses of UHPFRC strips used for strengthening the structures are as shown in the Figs. 25 and 26 respectively.

From the Figs. 25 and 26, it can be inferred that the lateral load carrying capacities of the structure increased as the thickness of the strip increased. The first failure loads of different components of the structure when subjected to this lateral load is obtained as shown in the Fig. 27.

It can be inferred that the strengthening material is more ductile when compared with normal concrete as its failure load is higher. The failure patterns in the structures with and without strengthening observed by applying the lateral load are as shown in the Fig. 28.

In all cases, cracks in concrete first initiated at the base of the column and these cracks propogated through the column. Later the strip cracked at a certain point of time and the complete column failed after the strip and the column concrete cracked. These cracks propogated to the beam column joints and the concrete at these points also cracked simultaneously. Steel yielded at the base of the column and the beam column joints resulting in the complete failure of the structure.

9.2 Analyzing the RC frame with beam column joints strengthened using UHPFRC strip

The beam column joints in case of both GLDS and ELDS are strengthened with UHFRC strips of 10 mm and 20 mm thicknesses. The length of these strips in each direction is taken as a trial length equal to one-fourth of the length of each member of the structure to which it is attached. The UHPFRC strengthening strip, assembly of the

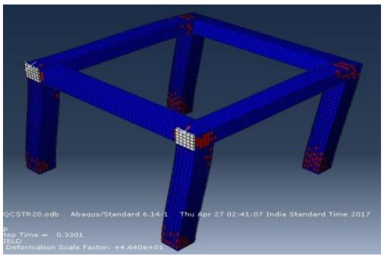

Fig. 28 Failure patterns in concrete of the structures after column strengthening

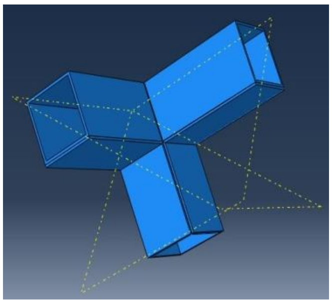

Fig. 29 Shape of UHPFRC strip used for beam column joint strengthening

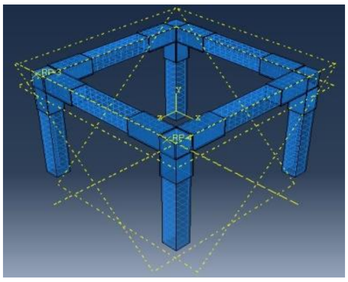

Fig. 30 Assembly of UHPFRC with the structures

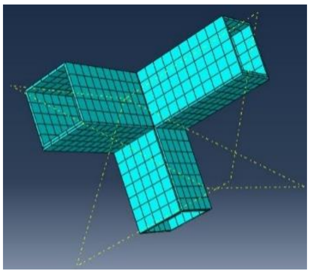

Fig. 31 Meshing the UHPFRC strip

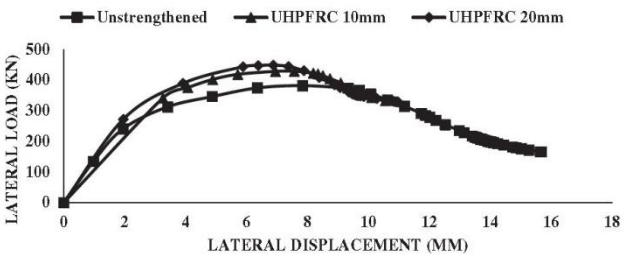

Fig. 32 Lateral load vs. displacement behavior of GLDS before and after beam column joint strengthening

strip with the structure and the mesh details of the strip used are as shown in the Figs. 29-31 respectively.

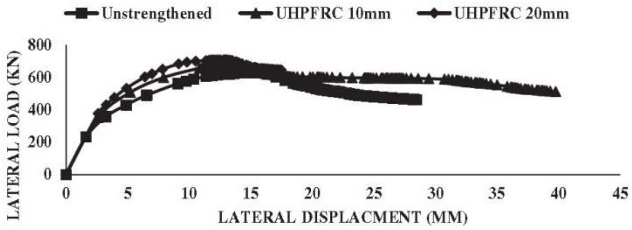

Fig. 33 Lateral Load vs. Displacement behavior of ELDS before and after beam column joint strengthening

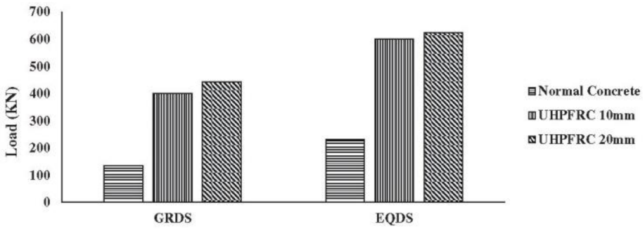

Fig. 34 First failure loads of materials in structures after beam column joint strengthening

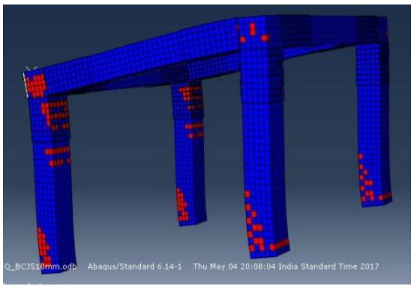

Fig. 35 Failure patterns in concrete of the structures after beam column joint strengthening

The lateral load vs. displacement behavior of GLDS and ELDS for different thicknesses of UHPFRC strips used for strengthening the structures are as shown in the Figs. 32 and 33.

The lateral load carrying capacities of the structures increased as the thickness of the strip used for strengthening the beam column joint increased. The first failure loads of different components of the structures when subjected to this **lateral load** is as shown in the Fig. 34.

It can be observed that UHPFRC is more ductile when compared with that of normal concrete because of its higher failure load which is same as in the case of column strengthening. The failure patterns of the structures observed after strengthening are as shown in the Fig. 35.

Cracks in concrete initiated at the base of the column and then propogated through the column concrete. Then a crack initiated at the center of the UHPFRC strip. The cracks in the strip propogated and the strip failed completely after a certain point of time. Later, these cracks propogated towards the beam column joint of the structures resulting in the failure of the beam column joint completely.

10. Comparing the efficiency of strengthening

A comparision is made to test the efficiency of two

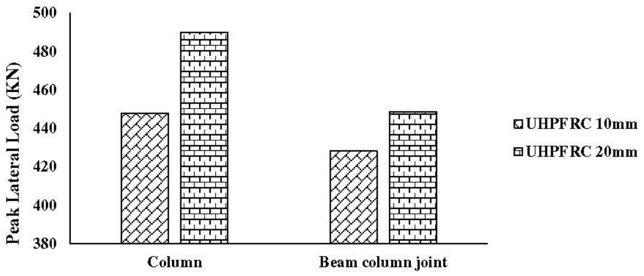

Fig. 36 Peak lateral loads of GLDS with both the strengthening locations

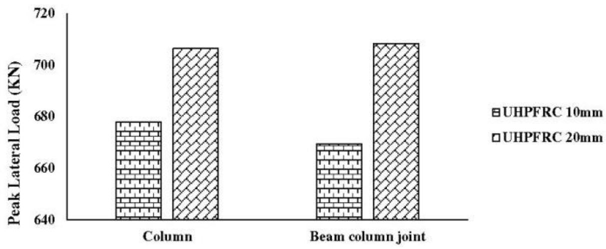

Fig. 37 Peak lateral loads of ELDS with both the strengthening locations

strengthening procedures i.e., the column and the beam column joint. This efficiency evaluation is performed based on the improvement in the peak lateral loads of the structures. The results obtained are as shown in the Figs. 36 and 37.

In case of GLDS, it can be noted that the column strengthening showed better improvement in the peak lateral load than the beam column joint strengthening for both the thicknesses of the strips used. But in the case of ELDS, column strengthening with 10 mm strip is better and in the case of strengthening with 20 mm strip the peak lateral loads obtained are almost similar irrespective of the type of strengthening method used.

11. Conclusions

1. From the results obtained it can be concluded that the CDP model worked out well in predicting the behavior of RC frames subjected to vertical and lateral loads.
2. UHPFRC can be successfully used to improve the lateral load carrying capacities of RC frames.
3. With the increase in the thickness of the UHPFRC strip, the load carrying capacity of the frame also increased accordingly for both GLDS and ELDS.
4. The first failure loads of different components are higher in the case of ELDS when compared with GLDS due to higher ductility.
5. UHPFRC used for strengthening the structure is more ductile when compared to normal concrete as the first failure loads are higher in the case of strengthened specimens.
6. Column strengthening is found to be better as the lateral load carrying capacities of the structures improved by more than 3% when this technique is used. Beam column joint strengthening might also work out if the length of the strip used for strengthening is increased which is not practically advisable.

References

Ali Shah, S.A., Shahzads, K., Afzal, S., Shabab, M.E. and Khattak, N. (2013), "Behaviour of infill walls under lateral loads in reinforced concrete frames-A review", *Int. J. Adv. Struct. Geotech. Eng.*, **2**(3), 106-109.

Ashish, U.K. and Harshalata, R. (2014), "Investigation on behaviour of reinforced concrete beam column joints retrofitted with FRP wrapping", *Int. J. Civil Eng. Res.*, **5**(3), 2278-3652.

Chalioris, C.E. (2013), "Steel fibrous RC beams subjected to cyclic deformations under predominant shear", *Eng. Struct.*, **49**, 104-118. https://doi.org/10.1016/j.engstruct.2012.10.010.

Chalioris, C.E. and Panagiotopoulos, T.A. (2018), "Flexural analysis of steel fibre-reinforced concrete members", *Comput. Concrete*, **22**(1), 11-25. https://doi.org/10.12989/cac.2018.22.1.011.

Chalioris, C.E. and Sfiri, E.F. (2011), "Shear performance of steel fibrous concrete beams", *Procedia Eng.*, **14**, 2064-2068. https://doi.org/10.1016/j.proeng.2011.07.259.

Chen, L. and Graybeal, B.A. (2011), "Modeling structural performance of ultrahigh performance concrete I-girders", *J. Bridge Eng.*, **17**(5), 754-764. https://doi.org/10.1061/(ASCE)BE.1943-5592.0000305.

Ermiao, L.I.N. and Pankaj, P. (2004), "Nonlinear static and dynamic analyses-The influence of material modeling In reinforced concrete frame structures", *Proceedings of the 13th World Conference on Earthquake Engineering*, Vancouver, BC, Canada.

Fadwa, I., Ali, T.A., Nazih, E. and Sara, M. (2014), "Reinforced concrete wide and conventional beam-column connections subjected to lateral load", *Eng. Struct.*, **76**, 34-48. https://doi.org/10.1016/j.engstruct.2014.06.029.

Genikomsou, S. and Polak, M. (2015), "Finite element analysis of punching shear of concrete slabs using damaged plasticity model in ABAQUS", *Eng. Struct.*, **98**, 38-48. https://doi.org/10.1016/j.engstruct.2015.04.016.

Jankowiak, T. and Lodygowski, T. (2005), "Identification of parameters of concrete damage plasticity constitutive model", *Found. Civil Environ. Eng.*, **6**(1), 53-69.

Kalyana Rama, J.S., Chauhan, D.R., Sivakumar, M.V.N., Vasan, A. and Murthy, A.R. (2017), "Fracture properties of concrete using damaged plasticity model-A parametric study", *Struct. Eng. Mech.*, ***64***(1), 59-69. https://doi.org/10.12989/sem.2017.64.1.059.

Lampropoulos, A.P., Paschalis, S.A., Tsioulou, O.T. and Dritsos, S.E. (2016), "Strengthening of reinforced concrete beams using ultra high performance fibre reinforced concrete (UHPFRC)", *Eng. Struct.*, **106**, 370-384. https://doi.org/10.1016/j.engstruct.2015.10.042.

Michal, S. and Winnicki, (2015), "Numerical simulations of corners in RC frames using Strut-and-Tie method and CDP model", *Proceedings of the XIII International Conference on Computational Plasticity: Fundamentals and Applications*, CIMNE ed. Barcelona, 608-619

Prem, P.R., Murthy, A.R., Ramesh, G., Bharatkumar, B.H. and Iyer, N.R. (2015), "Flexural behaviour of damaged rc beams strengthened with ultra high performance concrete", *Adv. Struct. Eng.*, 2057-2069. https://doi.org/10.1007/978-81-322-2187-6_158.

Rahman, S., Molyneaux, T. and Patnaikuni, I. (2005), "Ultra high performance concrete: recent applications and research", *Austr. J. Civil Eng.*, **2**(1), 13-20.

https://doi.org/10.1080/14488353.2005.11463913.
Sümer, Y. and Aktaş, M. (2015), "Defining parameters for concrete damage plasticity model", *Challenge*, **1**(3), 149-155.
Tayeh, B.A., Bakar, B.A., Johari, M.M. and Voo, Y.L. (2013), "Utilization of ultra-high performance fibre concrete (UHPFC) for rehabilitation-a review", *Procedia Eng.*, **54**, 525-538. https://doi.org/10.1016/j.proeng.2013.03.048.
Truong, G.T., Kim, J.C. and Choi, K.K. (2017), "Seismic performance of reinforced concrete columns retrofitted by various methods", *Eng. Struct.*, **134**, 217-235. https://doi.org/10.1016/j.engstruct.2016.12.046.
Tsonos, A.G. (2009), "Steel fiber high-strength reinforced concrete: a new solution for earthquake strengthening of old R/C structures", *WIT Tran. Built Environ.*, **104**, 153-164.
Tsonos, A.G. (2009), "Ultra-high-performance fiber reinforced concrete: an innovative solution for strengthening old R/C structures and for improving the FRP strengthening method", *WIT Tran. Eng. Sci.*, **64**, 273-284.

CC